Neutron-Spin Resonance in the Optimally Electron-Doped Superconductor $Nd_{1.85}Ce_{0.15}CuO_{4-\delta}$

Jun Zhao,[1] Pengcheng Dai,[1,2,*] Shiliang Li,[1] Paul G. Freeman,[3] Y. Onose,[4] and Y. Tokura[4,5]

[1]*Department of Physics and Astronomy, The University of Tennessee, Knoxville, Tennessee 37996-1200, USA*
[2]*Neutron Scattering Sciences Division, Oak Ridge National Laboratory, Oak Ridge, Tennessee 37831-6393, USA*
[3]*Institut Laue-Langevin, 6, rue Jules Horowitz, BP156-38042 Grenoble Cedex 9, France*
[4]*Spin Superstructure Project, ERATO, Japan Science and Technology, Tsukuba 305-8562, Japan*
[5]*Department of Applied Physics, University of Tokyo, Tokyo 13-8656, Japan*

(Received 27 March 2007; published 5 July 2007)

We use inelastic neutron scattering to probe magnetic excitations of an optimally electron-doped superconductor $Nd_{1.85}Ce_{0.15}CuO_{4-\delta}$ above and below its superconducting transition temperature $T_c = 25$ K. In addition to gradually opening a spin pseudogap at the antiferromagnetic ordering wave vector $\mathbf{Q} = (1/2, 1/2, 0)$, the effect of superconductivity is to form a resonance centered also at $\mathbf{Q} = (1/2, 1/2, 0)$ but at energies above the spin pseudogap. The intensity of the resonance develops like a superconducting order parameter, similar to those for hole-doped superconductors and electron-doped $Pr_{0.88}LaCe_{0.12}CuO_4$. The resonance is therefore a general phenomenon of cuprate superconductors, and must be fundamental to the mechanism of high-T_c superconductivity.

DOI: 10.1103/PhysRevLett.99.017001 PACS numbers: 74.72.Jt, 61.12.Ld, 75.25.+z

In conventional Bardeen-Cooper-Schrieffer (BCS) superconductors, the superconducting phase forms when electrons are bound into pairs with long-range phase coherence through interactions mediated by lattice vibrations (phonons) [1]. Since high-transition-temperature (high-T_c) superconductivity arises in copper oxides when sufficient holes or electrons are doped into the CuO_2 planes of their insulating antiferromagnetic (AFM) parent compounds [2], it is important to determine if spin fluctuations play a fundamental role in the mechanism of high-T_c superconductivity [3]. For hole-doped superconductors, it is now well documented that the spin fluctuations spectrum forms an ''hourglass'' dispersion with the most prominent feature, a collective excitation known as the neutron-spin resonance or resonance mode, centered at the AFM ordering wave vector $\mathbf{Q} = (1/2, 1/2)$ [4–14]. Although the energy of the mode tracks T_c and its intensity behaves like an order parameter below T_c for materials such as $YBa_2Cu_3O_{6+x}$ (YBCO) [4–8], the intensity of the saddle point where the low-energy incommensurate spin fluctuations merge into the commensurate $\mathbf{Q} = (1/2, 1/2)$ point in $La_{2-x}(Sr, Ba)_xCuO_4$ (LSCO) displays negligible changes across T_c [12–14]. Instead, the effect of superconductivity in optimally hole-doped LSCO is to open a spin gap [10] and pile density of states along incommensurate wave vectors at energies above the spin gap [11,13,14], and thus appears to be different from YBCO.

If the resonance is fundamental to the mechanism of superconductivity, it should be ubiquitous to all high-T_c superconductors. Although the superconductivity-induced enhancement at incommensurate wave vectors in LSCO has been argued to be comparable to the commensurate resonance in YBCO [15], the intensity gain of the resonance below T_c may not always be compensated by opening of a spin gap and spectral weight loss at lower energies. For example, the resonance intensity gain in the electron-doped $Pr_{0.88}LaCe_{0.12}CuO_4$ (PLCCO) ($T_c = 24$ K) below T_c is not compensated by spectral weight loss at lower energies [16]. On the other hand, while neutron scattering measurements found a low-temperature spin gap (about 4 meV) in the electron-doped superconductor $Nd_{1.85}Ce_{0.15}CuO_4$ (NCCO) [17,18], there have been no reports of the resonance or spectral weight gain at energies above the spin gap below T_c. Therefore, the relationship between the superconducting spin gap and the resonance is still an open question.

In this Letter, we report the results of inelastic neutron scattering studies of temperature dependence of the spin fluctuations in an optimally electron-doped NCCO ($T_c = 25$ K). We confirm the presence of a low-temperature spin (pseudo)gap [18] and show that the effect of superconductivity also induces a resonance at energies similar to electron-doped PLCCO [16]. Our results thus demonstrate that the resonance is a ubiquitous feature of optimally electron-doped superconductors. Its intensity gain below T_c in NCCO is due in part to the opening of a spin pseudogap and spectral weight loss at low energies. This is remarkably similar to the optimally hole-doped LSCO [13,14], and thus suggests that the enhancement at incommensurate wave vectors below T_c in LSCO has the same microscopic origin as the commensurate resonance in other high-T_c superconductors.

We grew a high-quality (mosaicity $<1°$, 3.5 g) NCCO single crystal using a mirror image furnace [19]. Figure 1(a) plots the magnetic susceptibility measurements showing an onset T_c of 25 K with a transition width of 3 K. Our neutron scattering experiments were performed on the IN-8 thermal triple-axis spectrometer at the Institute Laue-Langevin, Grenoble, France. We define the wave vector $\mathbf{Q}$ at (q_x, q_y, q_z) as $(h, k, l) = (q_x a/2\pi, q_y a/2\pi, q_z c/2\pi)$ re-

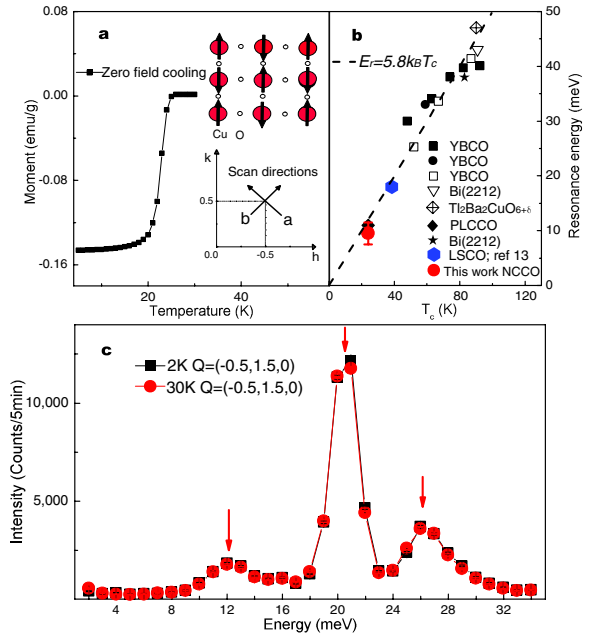

FIG. 1 (color online). (a) Schematic diagrams of real and reciprocal space of the CuO_2 with the transverse and longitudinal scans marked as a and b, respectively. Magnetic susceptibility measurements of T_c. (b) Summary of the resonance energy as a function of T_c for various hole- and electron-doped superconductors from [16] with NCCO (this work) and LSCO [13] added. (c) Energy scans at $\mathbf{Q} = (-0.5, 1.5, 0)$ at 2 and 30 K. The three CEF levels are marked by arrows [20].

ciprocal lattice units (r.l.u) in the tetragonal unit cell of NCCO (space group $I4/mmm$, $a = 3.95$, and $c = 12.07$ Å). For the experiment, the NCCO sample is mounted in the $[h, k, 0]$ zone inside a cryostat. We chose a focusing Si(111) as monochromator and PG(002) as analyzer without collimation. The final neutron energy was fixed at $E_f = 14.7$ meV with a pyrolytic graphite (PG) filter in front of the analyzer. This setup resulted an energy resolution of about 1 meV in FWHM at $\mathbf{Q} = (-0.5, 0.5, 0)$.

To understand the effect of superconductivity on the Cu^{2+} spin fluctuations, we must first determine the temperature dependence of the magnetic excitations from Nd^{3+} crystal electric field (CEF) levels in NCCO. For Nd ions in the tetragonal NCCO crystal structure, the three lowest energy CEF magnetic excitations are at $\hbar\omega = 12.2 \pm 0.3$, 20.3 ± 0.1, and 26.5 ± 0.3 meV [20]. Our energy scans at $\mathbf{Q} = (-0.5, 1.5, 0)$ confirm these results and show that the intensities of these CEF levels have small temperature dependence between 2 and 30 K [Fig. 1(c)].

Figure 2 summarizes the transverse and longitudinal (the scan directions are perpendicular and along $\mathbf{Q}$, respectively) $\mathbf{Q}$ scans around $(-0.5, 0.5, 0)$ at different energy transfers and temperatures. Consistent with earlier results on NCCO [18] and PLCCO [16,21], the scattering is commensurate and centered at $\mathbf{Q} = (-0.5, 0.5, 0)$ for all energies probed. Figures 2(a)–2(d) show the raw data (with scan directions marked) below and above T_c at $\hbar\omega =$

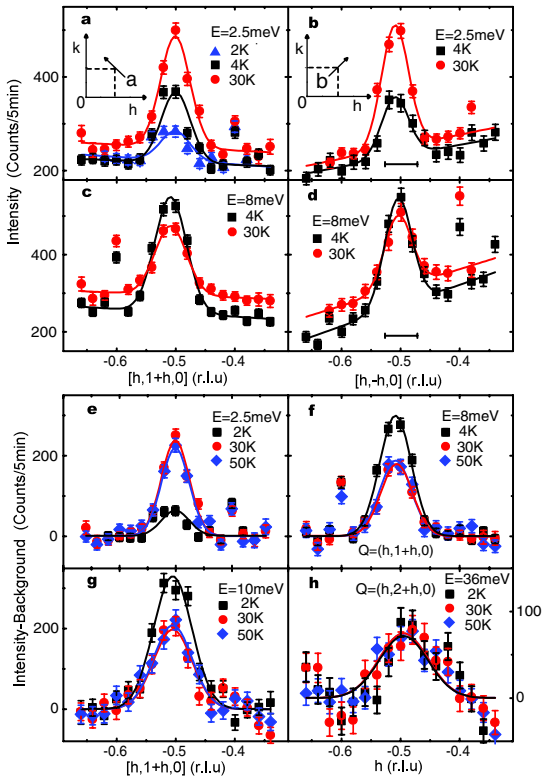

FIG. 2 (color online). Transverse and radial scans through $\mathbf{Q} = (-0.5, 0.5, 0)$ for (a),(b) $\hbar\omega = 2.5$ meV and (c),(d) 8 meV at various temperatures. Radial scans in (b),(d) are instrumental resolution limited (horizontal bars) that gives a minimum dynamic spin correlation length $\xi \approx 46$ Å at 2.5 meV. Transverse scans around $\mathbf{Q} = (-0.5, 0.5, 0)$ with linear background subtracted for (e) $\hbar\omega = 2.5$ meV, (f) 8 meV, and (g) 10 meV at temperature above and below T_c. (h) The transverse scan around $\mathbf{Q} = (-0.5, 1.5, 0)$ at $\hbar\omega = 36$ meV has negligible temperature dependence across T_c.

2.5, 8 meV. At $T = 30$ K ($T_c + 5$ K), the magnetic scattering above the linear backgrounds decreases slightly with increasing energy from 2.5 to 8 meV [Figs. 2(e) and 2(f)]. On cooling to below T_c, the peak intensity is drastically suppressed for $\hbar\omega = 2.5$ meV [Figs. 2(a) and 2(b)], and it increases for $\hbar\omega = 8$ meV [Figs. 2(c) and 2(d)]. Figures 2(e)–2(g) show background subtracted transverse scans at various energies. It is immediately clear that cooling below T_c suppresses the $\mathbf{Q} = (-0.5, 0.5, 0)$ peak at $\hbar\omega = 2.5$ meV but enhances scattering at $\hbar\omega = 8$ and 10 meV. On the other hand, magnetic scattering at $\hbar\omega = 36$ meV changes negligibly from 2 to 50 K [Fig. 2(h)].

Figures 3(a) and 3(b) show energy scans at the signal [$\mathbf{Q} = (-0.5, 0.5, 0)$] and background [$\mathbf{Q} = (-0.34, 0.66, 0)$] positions above and below T_c. Although the large Nd^{3+} CEF level dominated the magnetic scattering at $\hbar\omega = 12$ meV [20], one can still see clear Cu^{2+} spin fluctuations centered at $(-0.5, 0.5, 0)$ for energies between 2 and 10 meV. In the normal state, the magnetic scattering decreases with increasing energy, consistent with $\mathbf{Q}$ scans at $\hbar\omega = 2.5$, 8, and 10 meV [Figs. 2(e)–2(g)]. In the

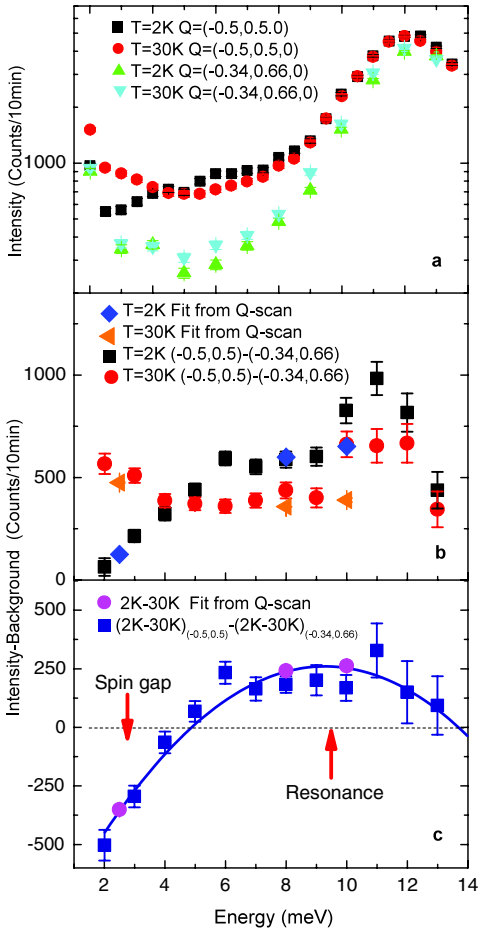

FIG. 3 (color online). (a) The temperature dependence of the scattering at the peak [$\mathbf{Q} = (-0.5, 0.5, 0)$] and background [$\mathbf{Q} = (-0.34, 0.66, 0)$] positions below and above T_c. Note the intensity is plotted in log scale to display the large intensity difference between the Nd^{3+} CEF level at $\hbar\omega = 12$ meV and Cu^{2+} spin fluctuations centered at $\mathbf{Q} = (-0.5, 0.5, 0)$ for energies between 2 and 10 meV. (b) Background subtracted magnetic scattering at $\mathbf{Q} = (-0.5, 0.5, 0)$ below and above T_c. The data are cross-checked by constant-energy scans in Fig. 2. (c) The temperature difference plot showing the resonance at $E_r = 9.5 \pm 2$ meV. The large error is due to the uncertainty in obtaining Cu^{2+} magnetic signal above 10 meV.

superconducting state, the low-energy spin fluctuations at $\mathbf{Q} = (-0.5, 0.5, 0)$ are suppressed for $\hbar\omega \leq 4$ meV and there is a clear scattering intensity gain for $6 \leq \hbar\omega \leq 10$ meV. The contrast between the normal and superconducting states becomes more obvious when changes in background scattering are taken into account [Fig. 3(b)]. The large Nd^{3+} CEF scattering between $10 < \hbar\omega < 33$ meV [Fig. 1(c)] overwhelmed Cu^{2+} magnetism. The background corrected difference plot between the superconducting and normal states shows a resonance at $\hbar\omega = 9.5 \pm 2$ meV, similar to that for PLCCO [16].

To determine if the low-temperature spin fluctuations' suppression below 4 meV and enhancement between 6 to 10 meV are indeed associated with the opening of a superconducting gap below T_c as in the tunneling experiments [22], we carefully measured the temperature dependent scattering at the peak [$\mathbf{Q} = (-0.5, 0.5, 0)$] and background positions for $\hbar\omega = 2.5$ and 8 meV (see Fig. 4). From previous low-energy inelastic neutron scattering work on NCCO [18], we know that the spin gap in NCCO opens gradually with decreasing temperature until it reaches about 4 meV at 2 K. While peak intensity in the $\mathbf{Q}$ scans at $\hbar\omega = 2.5$ meV show a clear low-temperature suppression, there is still a peak present at $\mathbf{Q} = (-0.5, 0.5, 0)$ even at 2 K. Therefore, optimally electron-doped NCCO does not have a clean spin gap as in the case of the optimally

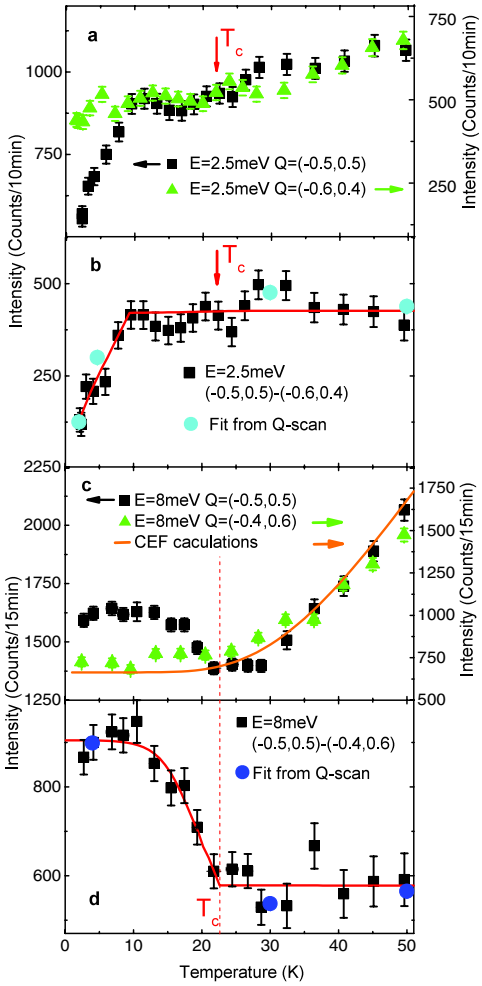

FIG. 4 (color online). Temperature dependence of the scattering at $\hbar\omega = 2.5$ and 8 meV. (a) The raw data at the signal [$\mathbf{Q} = (-0.5, 0.5, 0)$] and background [$\mathbf{Q} = (-0.6, 0.4, 0)$] positions. (b) The background subtracted magnetic scattering at $\hbar\omega = 2.5$ meV shows no anomaly across T_c but drops dramatically below 9 K. The data from the fitted $\mathbf{Q}$ scans are shown as circles. (c) Temperature dependent data for $\hbar\omega = 8$ meV with background at $\mathbf{Q} = (-0.4, 0.6, 0)$, a resonance coupled to T_c like an order parameter is clearly seen in the background subtracted data in (d). The estimated temperature dependence of the Nd^{3+} CEF level at 8 meV (from 12 to 20 meV) is shown as solid line in (c) [20].

hole-doped LSCO [10]. The temperature dependence of the scattering at the peak and background positions [Figs. 4(a) and 4(b)] reveals that the intensity suppression at $\hbar\omega = 2.5$ meV does not happen at T_c but at 9 K ($T_c - 16$ K). While this result confirms the earlier report [18], it also suggests that the gradual opening of the (pseudo) spin gap is not directly related the temperature dependence of the superconducting gap which is BCS-like [22] and becomes essentially fully opened with $2\Delta \approx 7$ meV below 12 K (50% of T_c).

On the other hand, the temperature dependence of the scattering at $\hbar\omega = 8$ meV is clearly coupled to the occurrence of superconductivity. With increasing temperature, the scattering at $\mathbf{Q} = (-0.5, 0.5, 0)$ first decreases like an order parameter, showing a kink at T_c, and then increases again above 30 K. It turns out that the large intensity rise above 30 K at $\hbar\omega = 8$ meV is due to the CEF transition from 12 to 20 meV as the 12 meV state is being populated with increasing temperature [Fig. 4(c)] [20]. As the CEF levels are weakly $\mathbf{Q}$ dependent, the large intensity increase above 30 K is also seen in the background [Fig. 4(c)]. The difference between signal and background shows a clear order-parameter-like temperature dependence of the resonance, remarkably similar to the temperature dependence of the resonance in PLCCO [16] and hole-doped superconductors [4–9]. Work is currently in progress to compare the magnetic scattering in NCCO and PLCCO using known phonons.

The observation of the resonance in another class of electron-doped superconductors suggests that the mode is a general phenomenon of electron-doped superconductors independent of their differences in rare-earth substitutions [17]. For hole-doped LSCO [10–14], the intensity enhancement in spin susceptibility above the spin-gap energy has been characterized as the magnetic coherence effect [11,15]. The observation of the susceptibility enhancement at energies ($6 \leq \hbar\omega \leq 13$ meV) just above the spin pseudogap energy of 4 meV in NCCO is consistent with this picture, although the temperature dependence of the spin pseudogap in NCCO behaves rather differently from those in LSCO [10,18]. In our search for the excitations responsible for electron pairing and high-T_c superconductivity, one of the arguments against the relevance of the resonance has been the inability to observe superconductivity-induced commensurate resonance in LSCO [10–14]. If the resonance is a phenomenon associated with the opening of a superconducting gap and the subsequent local susceptibility enhancement, it is natural to regard the susceptibility gain in both NCCO and LSCO as the resonance. Adding these two points to the universal $E_r = 5.8 k_B T_c$ plot in Fig. 1(b) suggests that while the resonance energy itself is intimately related to T_c, other details such as the spin gap, commensurability, and hourglass dispersion found in different materials may not be fundamental to the superconductivity.

For hole-doped superconductors, the hourglass dispersion has been interpreted either as the signature of "stripes" where doped holes are phase separated from the Mott-like AFM background [23–25] or as a bound state (spin exciton) within the gap formed in the noninteracting particle-hole continuum of a Fermi liquid [26,27]. Although the resonance in PLCCO has been interpreted as an overdamped spin exciton [28], it remains a challenge to understand how the resonance can arise both from NCCO which has a spin pseudogap and from the gapless PLCCO [29]. Since the resonance appears to be a general feature of optimally doped superconducting copper oxides, it must be understood in the microscopic theory for high-T_c superconductivity.

We thank Stephen Wilson and Jeff Lynn for earlier experiments on NCCO at NIST. This work is supported by the U.S. DOE BES under Grant No. DE-FG02-05ER46202. ORNL is supported by U.S. DOE No. DE-AC05-00OR22725 with UT/Battelle LLC.

*daip@ornl.gov

[1] J. Bardeen, L. N. Cooper, and J. R. Schrieffer, Phys. Rev. **108**, 1175 (1957).
[2] M. A. Kastner *et al.*, Rev. Mod. Phys. **70**, 897 (1998).
[3] D. J. Scalapino, Science **284**, 1282 (1999).
[4] J. Rossat-Mignod *et al.*, Physica (Amsterdam) **185C**, 86 (1991).
[5] H. F. Fong *et al.*, Phys. Rev. B **61**, 14 773 (2000).
[6] Pengcheng Dai *et al.*, Phys. Rev. B **63**, 054525 (2001).
[7] H. Woo *et al.*, Nature Phys. **2**, 600 (2006).
[8] C. Stock *et al.*, Phys. Rev. B **71**, 024522 (2005).
[9] H. F. Fong *et al.*, Nature (London) **398**, 588 (1999).
[10] K. Yamada *et al.*, Phys. Rev. Lett. **75**, 1626 (1995).
[11] T. E. Mason *et al.*, Phys. Rev. Lett. **77**, 1604 (1996).
[12] J. M. Tranquada *et al.*, Nature (London) **429**, 534 (2004).
[13] N. B. Christensen *et al.*, Phys. Rev. Lett. **93**, 147002 (2004).
[14] B. Vignolle *et al.*, Nature Phys. **3**, 163 (2007).
[15] J. M. Tranquada *et al.*, Phys. Rev. B **69**, 174507 (2004).
[16] S. D. Wilson *et al.*, Nature (London) **442**, 59 (2006).
[17] Y. Tokura, H. Takagi, and S. Uchida, Nature (London) **337**, 345 (1989).
[18] K. Yamada *et al.*, Phys. Rev. Lett. **90**, 137004 (2003).
[19] H. J. Kang *et al.*, Nature (London) **423**, 522 (2003).
[20] A. T. Boothroyd *et al.*, Phys. Rev. B **45**, 10 075 (1992).
[21] S. D. Wilson *et al.*, Phys. Rev. B **74**, 144514 (2006).
[22] L. Shan *et al.*, Phys. Rev. B **72**, 144506 (2005).
[23] S. A. Kivelson *et al.*, Rev. Mod. Phys. **75**, 1201 (2003).
[24] J. Zaanen *et al.*, Philos. Mag. B **81**, 1485 (2001).
[25] M. Vojta, T. Vojta, and R. K. Kaul, Phys. Rev. Lett. **97**, 097001 (2006).
[26] I. Eremin *et al.*, Phys. Rev. Lett. **94**, 147001 (2005).
[27] M. Eschrig, Adv. Phys. **55**, 47 (2006).
[28] J.-P. Ismer *et al.*, arXiv:cond-mat/0702375 [Phys. Rev. Lett. (to be published)]; J. X. Li *et al.*, Phys. Rev. B **68**, 224503 (2003).
[29] F. Krüger *et al.*, arXiv:cond-mat/07054424.